SPECT Imaging of Neovascularization With 99mTc-3PRGD2 for Evaluating Early Response to Endostar Involved Therapies on Pancreatic Cancer Xenografts in Vivo

Xiaona Jin
Peking Union Medical College Hospital
Chengyan Dong
Siemens Healthcare China
Kun Zheng
PUMCH: Peking Union Medical College Hospital
Ximin Shi
Peking Union Medical College Hospital
Yu Liu
PUMCH: Peking Union Medical College Hospital
Li Huo
Peking Union Medical College Hospital
Fan Wang
Medical Isotopes Research Center,Peking University
Fang Li (lifang@pumch.cn)
Peking Union Medical College Hospital

Original research

Keywords: Endostar, 99mTc-3PRGD2, antiangiogenesis, Single photon emission computed tomography, microvessel density

DOI: https://doi.org/10.21203/rs.3.rs-142194/v1

Abstract

Background

Molecular imaging targeting angiogenesis is warranted for specific monitoring of molecular changes as early therapeutic effects via antiangiogenesis. We explore the predictive value of ^{99m}Tc-PEG$_4$-E[PEG$_4$-c(RGDfK)]$_2$ (^{99m}Tc-3PRGD$_2$) as an integrin αvβ3 targeting imaging agent for monitoring the efficacy of endostar antiangiogenic therapy and chemotherapy in an animal model, to find a specific pathway that could monitor early therapeutic effects.

Results

Tumor growth was significantly lower in treatment groups than in the control group (P<0.05), and also in Endostar + Gemcitabine group than in Endostar group(P=0.034) or Gemcitabine group (P=0.021), and the differences was observed at 28 days after treatment. The difference of uptake of 99mTc-3PRGD2 was observed between the control group and Endostar group(P=0.033) or the combination therapy group(P<0.01) at 7 days after treatment, and at 14 days after treatment between the control group and Gemcitabine group(P<0.01). ^{99m}Tc-3PRGD$_2$ accumulation was significantly correlated with microvessel density (r=0.998, P=0.002).

Conclusion

With ^{99m}Tc-3PRGD$_2$ SPECT, the tumor response to antiangiogenic therapy, chemotherapy, and combination therapy can be assessed at a very early stage of treatment, much earlier than the tumor volume change, which provides new opportunities to develop individualized therapeutic approaches and optimized dosages for effective treatments.

Introduction

Inhibition of angiogenesis can provoke vascular regression, impeding delivery of oxygen and nutrients, and ultimately starving the tumor. Antiangiogenic therapy has been approved by many countries as an effective strategy to inhibit tumor growth, providing a novel treatment approach for cancer patients [1-2]. As a recombinant human endostatin□Endostar , was mainly used as an antiangiogenic agent for cancer treatment [3-4], which was approved by the China Food and Drug Administration (CFDA) in 2005 for treatment of lung cancer. Endostar exhibits antiangiogenic effects and has been used to treat numerous types of cancer, including non-small lung, breast, melanoma tumor, and gastric cancer [5-10]. Nevertheless, the benefits of Endostar on pancreatic cancer are currently poorly known. Endostar combined with temozolomide or dacarbazine + 5-FU was effective in the treatment of advanced pancreatic neuroendocrine tumors, and the combinations were well tolerated[11]. A preclinical study revealed an unfavorable proangiogenic side effect of cantharidin via targeting the pancreatic cancer angiogenic microenvironment in vivo. Antiangiogenic therapeutics or inhibitors of proangiogenic kinase pathways could antagonize the growth-promoting effect of cantharidin and present additive antitumor effects, exhibiting adequate efficacy. As an antiangiogenic agent, Endostar showed good safety profile and tolerance in previous studies, without toxicities commonly seen with other VEGF or VEGFR inhibitors, such as hypertension and proteinuria [12-16].

In past years, clinical trials of anti-angiogenic therapy with anti-VEGF (bevacizumab) or anti-VEGFR (sorafenib, Axitinib) for pancreatic cancer, have been carried out [17-21]. As is often observed in clinical trials, patient responses are variable, with only a subset of patients benefiting from the therapy [22-23]. Therefore, it is in great demand to develop an alternative approach to identify patients who most likely benefit from antiangiogenic treatment, to detect emerging resistance, and to monitor early therapeutic efficacy [24].

As a prognostic indicator of progression, histopathologic evaluation of microvessel density (MVD) is not practical for routinely evaluating tumor angiogenesis because of its invasive nature of the procedure [25]. Noninvasive imaging technologies such as dynamic contrast-enhanced (DCE) magnetic resonance imaging (MRI) or computed tomography (CT), used to provide evidence on tumor blood flow, permeability, and volume, are technically challenging and cannot directly and effectively quantify the changes of post-treatment tumoral vascularity [26–28]. Positron emission tomography (PET) using ^{18}F-FDG (2-deoxy-2-18F-fluoro-D-glucose) also was used to monitor antiangiogenic therapy by determining glucose metabolism changes, but it may not be an ideal modality because it is not a tumor-specific radiotracer. Therefore, molecular imaging targeting specific pathways involved in angiogenesis is

warranted for specific monitoring of some molecular changes as early therapeutic effects via antiangiogenesis, with the benefit that it allows repetitive noninvasive follow-ups during the course of therapy.

Imaging integrin $\alpha_v\beta_3$ may provide new opportunities to document tumor angiogenesis and monitor response to antiangiogenesis treatment [29]. The Arg-Gly-Asp (RGD) sequence has been known to bind with the integrin αvβ3 that is expressed on the surface of angiogenic blood vessels or tumor cells [30]. Thus, various radiolabeled derivatives of RGD peptides have been developed for angiogenesis imaging by positron emission tomography (PET) imaging, such as ^{18}F- $FPRGD_2$ and ^{68}Ga-NOTA-$PRGD_2$, and single-photon emission computed tomography (SPECT) imaging for the diagnosis of cancers, such as ^{99m}Tc-$3PRGD_2$ [31-35].

In our previous studies，high uptake of ^{99m}Tc-$3PRGD_2$ was observed in tumors of human pancreatic cancer xenograft model（PANC-1）and patients with pancreatic cancer, ^{99m}Tc-$3PRGD_2$ SPECT showed the value of the diagnosis of pancreatic cancer[36]. And now we try to investigate ^{99m}Tc-$3PRGD_2$ as an integrin $\alpha_v\beta_3$ targeting imaging agent for monitoring the efficacy of endostar antiangiogenic therapy and chemotherapy in an animal model，comparing with MVD，to find a specific pathway which could early monitor therapeutic effects and is applicable for follow-ups during therapy.

Methods

Radiopharmaceutical Preparation

Synthesis of the labeling precursor, kit preparation, and subsequent ^{99m}Tc-labeling were performed as previously described[35]. Briefly, the kit for the preparation of ^{99m}Tc-$3PRGD_2$ was formulated by combining 20mg of hydrazinonicotinamide-$3PRGD_2$, 5 mg of trisodium triphenylphosphine-3,39,399-trisulfonate (TPPTS), 6.5 mg of tricine, 40mg of mannitol, 38.5 mg of disodium succinate hexa- hydrate, and 12.7 mg of succinic acid. For ^{99m}Tc radiolabeling, to the kit vial was added 1 mL of 1,110–1,850 MBq (30–50 mCi) of $^{99m}TcO4^-$ saline solution, and then the vial was water-bathed at 100℃for 15–20 min. The resulting solution was analyzed by instant thin-layer chromatography using Gelman Sciences silica-gel paper strips and a 1:1 mixture of acetone and saline as eluant. The radiochemical purity was always greater than 95%. The reaction mixture was then diluted to approximately 370 MBq/mL (10 mCi/mL) with saline and was filtered with a 0.20-mm Millex- LG filter (EMD Millipore). Each animal was injected with 7.4-11.1 MBq (0.2-0.3 mCi) of ^{99m}Tc-$3PRGD_2$ per mice. The resulting solution was analyzed by instant thin-layer chromatography using paper strips and acetone as eluent. The radiochemical purity was >95%.

Animal Model Establishment.

Female BALB/c mice (5 weeks of age) were purchased from Vital River Lab Animal Technology Co., Ltd. PANC-1 mice model was established by subcutaneous injection of 2×10^6 PANC-1cells into the right rear legs of mice. Once the tumor diameter reached 5-7mm, the mice were initiated with treatment (2 weeks after inoculation of PANC-1cells).

Treatment Protocol.

The study flowchart is provided in Fig. 1. PANC-1 tumor-bearing BALB/c mice with a tumor size of 5-7mm were randomly assigned to four groups (n = 7 mice per group). The mice were randomly assigned to four major groups. The first group was injected 10 mg/kg of Endostar, the second one with 10 mg/kg of Gemcitabine, the third one with 10 mg/kg of Endostar and 10 mg/kg of Gemcitabine at the same time ,and the control group with 0.9% saline. The treatments were performed daily for 28 days continuously. Tumor dimensions were measured every day with digital calipers, and the tumor volume was calculated using the formula (volume = 1/2 length × width × width). To assess potential toxicity, body weight was measured daily. All mice were euthanized and the tumor tissues were harvested for further immunohistochemical staining when the treatment was complete.

Imaging Protocol

The scanner was dual-head g-cameras, using low-energy high-resolution collimators and a 20% energy window centered on 140 keV. After intravenous injection of ^{99m}Tc-$3PRGD_2$, static planar scans of the mice were obtained at 1.5h（the highest time point of tumor uptake）. The acquisition count was 3×10^5. The matrix is 256 × 256, and the magnification is 1.33. The region of interest

(ROI) of the tumor (T) and contralateral corresponding site (NT) were delineated, and the ratio of radioactivity (T/NT) was calculated. The study flowchart is provided in Fig. 1.

Immunofluorescence staining

Vascular endothelium was labeled using immunohistochemical staining with isolectin B4. The fluorescence staining study was carried out as previously described [37]. Slides were incubated with the fluorescein-labeled Griffonia Simplicifolia Lectin I (GSLI) Isolectin B4 (FL-1201, 1: 50, Vector Laboratories, USA) overnight at 4°C and sealed with DAPI Fluoromount-G® mounting medium (Southern Biotech, USA). Microvessel density was counted on the isolectin B4-stained slides in three fields in a blinded way using a fluorescence microscope in three fields under 40×magnification and the results were averaged.

Statistical Analysis

Quantitative and semiquantitative data were expressed as the mean ± SD and analyzed using SPSS version 17.0 (IBM, Chicago, IL, USA). Mean values were compared using one-way analysis of variance (ANOVA) or Student's t-test. Two-way repeated-measures analysis of variance (ANOVA) was used to evaluate the differences between different treatment groups.

Results

Effect of Treatments on Tumor Growth

The antiangiogenic therapy with Endostar, Gemcitabine, Endostar, and Gemcitabine were carried out in PANC-1 tumor-bearing mice. No significant tumor growth inhibition was observed in Endostar or Gemcitabine group as compared with the control group before day 21 post-treatment ($p > 0.05$). At the end of the therapeutic study (day 28 post-treatment), the tumor growth of the control group was rapid with the tumor sizes reaching over 1881±523 mm^3, but 1160±212 mm^3 in the Endostar group, 1171±496 mm^3 in the gemcitabine group, and 801±399 mm^3 ($P<0.05$), demonstrating the tumor growth inhibition effect of treatments. For the therapeutic effect evaluated by tumor volume, two-way repeated-measures ANOVA was statistically significant for differences between treatment groups and the control group shown in Table1Fig.2A. Tumor growth was significantly faster in controls than in all other groups ($P<0.05$) and in Endostar or Gemcitabine alone vs. Endostar + Gemcitabine ($P=0.034$ for Endostar and $P=0.021$ for Gemcitabine). Treatment was the only regimen that resulted in slowing tumor growth.

Monitoring the Efficacy of Antiangiogenic Therapy by SPECT.

For monitoring the efficacy of antiangiogenic therapy, SPECT imaging was performed by using ^{99m}Tc-3PRGD2 on before treatment and days 7, 14, 21, and 28 post-treatment, respectively. At baseline, the tumor uptake values (T/NT) of ^{99m}Tc-3PRGD$_2$ were 1.50 ± 0.08,1.50±0.17,1.52±0.11,1.55±0.19, and T/NT in treatment groups at this time was no significant difference compared to the control group. 7days after treatment, T/NT in the Endostar group was significantly lower than the control group (1.67 ± 0.16 vs 1.87±1.15, $P=0.033$), and the difference lasted until the end of treatment. The difference was also observed between the control group and the both of Endostar and Gemcitabine group. But there was no difference between the Gemcitabine group and the control group until 14 days after treatment. For the therapeutic effect evaluated by T/NT, two-way repeated-measures ANOVA was statistically significant for differences between treatment groups and the control group shown in Table2. T/NT raise was significantly faster in controls than in all other groups ($P<0.05$) and in Endostar or Gemcitabine alone vs. Endostar + Gemcitabine ($P=0.034$ for Endostar and $P=0.021$ for Gemcitabine), treatment was the only regimen that resulted in slowing the growth of the T/NTFig.2B

Immunohistochemical Findings

Twenty-eight specimens were stained with isolectin B4 to correlate with the imaging findings. The microvessel densityMVDwere 10.5±1.7,15.3±2.5,9.7±1.4,23.1±2.7 in each microscopic in the Endostar group, Gemcitabine group, both of Endostar and Gemcitabine group, the control group (Fig.3). ^{99m}Tc-3PRGD$_2$ accumulation was significantly correlated with MVD counted on the isolectin B4-stained slides($r=0.998$P=0.002). MVD in the treatment groups were was significantly lower than the control group$P<0.05$. The difference was observed between the Endostar group and the Gemcitabine groupbut there was no difference between the Endostar group and the both of Endostar and Gemcitabine.

Discussion

Pancreatic cancer remains one of the deadliest malignancies, responsible for substantial morbidity and mortality worldwide. The 5-year survival rate at the time of diagnosis is 10% in the USA and about 7% in China, as approximately 80–85% of patients present with either unresectable or metastatic disease [38-39]. Systemic chemotherapy combinations including FOLFIRINOX (5-fluorouracil, folinic acid [leucovorin], irinotecan, and oxaliplatin) and gemcitabine plus nab-paclitaxel remain the mainstay of treatment for patients with advanced disease [40]. Therefore, new effective therapeutic schemes and sensitive evaluation of curative effect by noninvasive imaging methods become very important. In addition to conventional chemotherapy combinations, multiple trials of anti-angiogenic therapy with anti-VEGF (bevacizumab), anti-VEGFR (sorafenib, Axitinib) or for pancreatic cancer, have been carried out with different results, some producing additional benefits [41-43]and others didn't [16-21] with different therapies. In our study, Endostar was chosen as an antiangiogenic drug for the treatment of pancreatic tumors on mouse pancreatic cancer xenografts alone or combined with Gemcitabine . And ^{99m}Tc-3PRGD$_2$ SPECT was used to evaluate the therapeutic effect targeting neovascularization.

The results of two-way repeated-measures ANOVA showed that the three therapeutic schemes were effective in inhibiting tumor growth. At the end of the 14 days, Endostar or Gemcitabine treatment didn't induce a significant reduction in the slope of tumor growth, as compared to controls. But the combination of Endostar and Gemcitabine the tumor volume of all the treated mice was significantly smaller than that of the control group. Until the end of 28 days of treatment in monotherapy groups the tumor growth was observed to be lower than that in the control group. In the Endostar-treated group, these results are explained by the mechanism of action of Endostar, which blocks the VEGF/VEGFR signaling pathway, it hampers tumor growth by mediating the regression of existing tumor vasculature and preventing regrowth over time [44-45]. But this agent is not able to eradicate the tumor all by itself [46]. In the Gemcitabine-treated group, chemotherapy created cytotoxic lesions resulting in an aberrant DNA repair leading to cell apoptosis. The combination of those two agents appeared to be more efficient thanks to their synergic action on two different pathways that promote tumor growth. It is now becoming increasingly clear that vascular normalization is associated with decreased tumor metastasis [47-48]. Jain and Lin and Sessa proposed the theories of "vascular normalization" and "window" successively [49-50]. They reported that following administration of the antiangiogenic agents, a unique "window" occurred, where irregular vessels inside the tumor were normalized. In recent years, it has been reported that Endostar can not only inhibit neovascularization, but also induce pathological vascular normalization which has shown great clinical potential for enhancing effective drug delivery, improving local immunosuppressive microenvironment, and reducing distant metastasis [51-52]. Therefore, Endostar may be a potential drug for anti-angiogenic therapy of pancreatic cancer.

At the end of the second week, a reduction in ^{99m}Tc-3PRGD$_2$ tumor uptake T/NT was observed in the mice treated with Endostar alone or combined with Gemcitabine, compared with control, in agreement with a reduction in tumor growth. At the end of the 14 days T/NT in the Gemcitabine group was significantly lower than the control group. The results of two-way repeated-measures ANOVA made sure that the treatment was the regimen that resulted in slowing the growth of the T/NT. Compared with the tumor volume, the difference of the T/NT between treatment groups and the control group was observed earlier. And also, the difference the of the T/NT in treatment groups including Endostar appeared earlier than in the Gemcitabine group. The possible reason may be that Endostar mediates the reduction of neovascularization earlier than Gemcitabine.

Endostar inhibited the newborn vascular endothelial cells, causing a decrease of integrin expression, which led to the decrease of integrin-targeted imaging probe uptake in the tumor. The reduction of neovascularization may also occur in the Gemcitabine. The findings were confirmed by immunofluorescence staining isolectin B4. MVD in all the treatment groups was significantly lower than the control group. MVD in the Gemcitabine group was higher than in the Endostar group and the combination of those two agents group, but no difference between the Endostar group and the combination of those two agents group that maybe because of Endostar reducing neovascularization more obviously than Gemcitabine. T/NT was significantly correlated with MVD. ^{99m}Tc-3PRGD$_2$ SPECT could be a noninvasive method for evaluating MVD.

There were some limitations in the study, The tumor is not very small for the convenience of imaging so a difference between the treatment groups and the control group came late. "vascular normalization" and "window" had not been studied, because the focus of our research is imaging to monitor therapeutic effects.

Conclusions

With ^{99m}Tc-3PRGD$_2$ SPECT, the tumor response to antiangiogenic therapy, chemotherapy and can be assessed at a very early stage of treatment, much earlier than the anatomical structure change by monitoring the tumor volume, which provides new opportunities to develop individualized therapeutic approaches and establish optimized dosages and dose intervals for an effective treatment that benefit patients.

Declarations

Ethics approval and consent to participate:

This study had been approved by the Institute Review Board of Peking Union Medical College Hospital, Chinese Academy of Medical Sciences & Peking Union Medical College.

Consent for publication:

Not applicable.

Availability of data and material:

The datasets used in the current study are available from the corresponding author on reasonable request.

Competing interests:

There is no conflict of interest.

Funding:

This work was financially supported, in part, by the National Natural Science Foundation of China (NSFC) projects (81601551、81801741、81671722).

Authors' contributions

LF, WF designed the study. LY, DC were responsible for radiosynthesis. ZK, SX were responsible for animal studies. HL helped in study supervision. The manuscript was drafted by JX and DC. All authors read and approved the final manuscript.

Acknowledgements

Not applicable.

Author details

1.Department of Nuclear Medicine, Peking Union Medical College Hospital, Chinese Academy of Medical Sciences and Peking Union Medical College, Beijing, 100730, China .2.GE Healthcare China, Beijing, 100176、China.3.Medical Isotopes Research Center, Peking University, Beijing 100191, China;

References

1. Burke, P. A.; DeNardo, S. J. Antiangiogenic agents and their promising potential in combined therapy. Rev. Oncol. Hemat. 2001, 39 (1–2), 155–171.
2. Folkman, J. Antiangiogenesis in cancer therapy: endostatin and its mechanisms of action. Exp. Cell Res. 2006, 312 (5), 594–607.
3. Ezzell, C. Starving tumors of their lifeblood. Sci. Am. 1998, 279 (4), 33–34.
4. Ge W, Cao DD, Wang HM, Jie FF, Zheng YF, Chen Y. Endostar combined with chemotherapy versus chemotherapy alone for advanced NSCLCs: a meta-analysis. Asian Pac J Cancer Prev. 2011;12(10):2705-2711.

5. Ling Y, Yang Y, Lu N, You QD, Wang S, Gao Y, et al. Endostar, a novel recombinant human endostatin, exerts antiangiogenic effect via blocking VEGF-induced tyrosine phosphorylation of KDR/Flk-1 of endothelial cells. Biochem Biophys Res Commun. 2007;361(1):79-84
6. Li Y, Huang XE, Yan PW, Jiang Y, Xiang J. Efficacy and safety of endostar combined with chemotherapy in patients with advanced solid tumors. Asian Pac J Cancer Prev. 2010;11(4):1119-1123.
7. Jia L, Ren S, Li T, Wu J, Zhou X, Zhang Y, et al. Effects of Combined Simultaneous and Sequential Endostar and Cisplatin Treatment in a Mice Model of Gastric Cancer Peritoneal Metastases. Gastroenterol Res Pract. 2017; doi: 10.1155/2017/2920384.
8. Xiao L, Yang S, Hao J, Yuan X, Luo W, Jiang L, et al.Endostar attenuates melanoma tumor growth via its interruption of b-FGF mediated angiogenesis. Cancer Lett. 2015;359(1):148-154.
9. Lu N, Ling Y, Gao Y, Chen Y, Mu R, Qi Q, et al: Endostar suppresses invasion through downregulating the expression of matrix metalloproteinase-2/9 in MDA-MB-435 human breast cancer cells. Exp Biol Med.2008;233(8):1013-1020.
10. Wen QL, Meng MB, Yang B, et al: Endostar, a recombined humanized endostatin, enhances the radioresponse for human nasopharyngeal carcinoma and human lung adenocarcinoma xenografts in mice. Cancer Sci.2009;100(8):1510-1519
11. Xu MD, Liu L, Wu MY, Jiang M, Shou LM, Wang WJ, et al. The combination of cantharidin and antiangiogenic therapeutics presents additive antitumor effects against pancreatic cancer. Oncogenesis. 2018 Nov 26;7(11):94.
12. Wang J, Sun Y, Liu Y, Yu Q, Zhang Y, Li K, et al. Results of randomized, multicenter, double- blind phase III trial of rh-endostatin (YH-16) in treatment of advanced non-small cell lung cancer patients [in Chinese]. Zhongguo Fei Ai Za Zhi .2005;8(4):283-90.
13. Han B, Xiu Q, Wang H, Shen J, Gu A, Luo Y, et al. A multicenter, randomized, double-blind, placebo-controlled study to evaluate the efficacy of paclitaxel-carbopla- tin alone or with endostar for advanced non-small cell lung cancer. J Thorac Oncol.2011;6:1104–1109.
14. Li Y, Huang XE, Yan PW, Jiang Y, Xiang J. Efficacy and safety of endostar combined with chemotherapy in patients with advanced solid tumors. Asian Pac J Cancer Prev. 2010;11(4):1119-23.
15. Zhang LP, Liao XY, Xu YM, Yan LJ, Yan GF, Wang XX, Duan YZ, Sun JG. Efficacy and safety of endostar® combined with chemotherapy in patients with advanced soft tissue sarcomas. Asian Pac J Cancer Prev. 2013;14(7):4255-4259.
16. Rong B, Yang S, Li W, Zhang W, Ming Z. Systematic review and meta-analysis of Endostar (rh-endostatin) combined with chemotherapy versus chemotherapy alone for treating advanced non-small cell lung cancer. World J Surg Oncol.2012;10:170.
17. Van Cutsem E, Vervenne WL, Bennouna J, Humblet Y, Gill S, Van Laethem JL, et al,Phase III trial of bevacizumab in combination with gemcitabine and erlotinib in patients with metastatic pancreatic cancer. J Clin Oncol.2009 ;27(13):2231-7.
18. Kindler HL, Niedzwiecki D, Hollis D, Sutherland S, Schrag D, Hurwitz H, et al.Gemcitabine plus bevacizumab compared with gemcitabine plus placebo in patients with advanced pancre- atic cancer: phase III trial of the Cancer and Leukemia Group B (CALGB 80303). J Clin Oncol.2010;28(22):3617–3622.
19. Kindler HL, Ioka T, Richel DJ, Bennouna J, Letourneau R, Oku- saka T, et al.Axitinib plus gemcitabine versus placebo plus gemcitabine in patients with advanced pancreatic adenocarci- noma: a double-blind randomised phase 3 study. Lancet Oncol.2011;12(3):256–262.
20. Goncalves A, Gilabert M, Francois E, Dahan L, Perrier H, Lamy R, et al. BAYPAN study: a double-blind phase III randomized trial comparing gemcitabine plus sorafenib and gemcitabine plus placebo in patients with advanced pancreatic cancer. Ann Oncol.2012;23(11):2799–2805.
21. Rougier P, Riess H, Manges R, Karasek P, Humblet Y, Barone C, et al. Randomised, placebo-controlled, double-blind, parallel-group phase III study evaluating aflibercept in patients receiving first- line treatment with gemcitabine for metastatic pancreatic cancer. Eur J Cancer.2013;49(12):2633–2642.
22. Sennino B, McDonald DM. Controlling escape from angiogenesis inhibitors. Nat Rev Cancer. 2012; 12: 699–709.
23. Scott BJ, Quant EC, McNamara MB, Ryg PA, Batchelor TT, Wen PY. Bevacizumab salvage therapy following progression in high-grade glioma patients treated with VEGF receptor tyrosine kinase inhibitors. Neuro Oncol. 2010; 12:603–607.
24. Sessa C, Guibal A, Del Conte G, Ruegg C. Biomarkers of angiogenesis for the development of antiangiogenic therapies in oncology: tools or decorations? Nat Clin Pract Oncol. 2008; 5:378–391.

25. Foote RL, Weidner N, Harris J, Hammond E, Lewis JE, Vuong T, et al. Evaluation of tumor angiogenesis measured with microvessel density (MVD) as a prognostic indicator in nasopharyngeal carcinoma: results of RTOG 9505. Int J Radiat Oncol Biol Phys. 2005; 61:745–753.
26. Morgan B, Thomas AL, Drevs J, Hennig J, Buchert M, Jivan A, et al. Dynamic contrast- enhanced magnetic resonance imaging as a biomarker for the pharmacological response of PTK787/ZK 222584, an inhibitor of the vascular endothelial growth factor receptor tyrosine kinases, in patients with advanced colorectal cancer and liver metastases: results from two phase I studies. J Clin Oncol. 2003; 21:3955–3964.
27. Akisik MF, Sandrasegaran K, Bu G, Lin C, Hutchins GD, Chiorean EG. Pancreatic cancer: utility of dynamic contrast- enhanced MR imaging in assessment of antiangiogenic therapy. Radiology. 2010; 256:441–449.
28. Bradley DP, Tessier JL, Checkley D, Kuribayashi H, Waterton JC, Kendrew J, et al. Effects of AZD2171 and vandetanib (ZD6474, Zactima) on haemodynamic variables in an SW620 human colon tumour model: an investigation using dynamic contrast-enhanced MRI and the rapid clearance blood pool contrast agent, P792 (gadomelitol). NMR Biomed. 2008; 21:42–52.
29. Haubner R, Wester HJ. Radiolabeled tracers for imaging of tumor angiogenesis and evaluation of anti-angiogenic therapies. Curr Pharm Des 2004;10(13):1439–1455.
30. Haubner R, Wester HJ, Reuning U.Radiolabeled αvβ3 integrin antagonists: A new class of tracers for tumor targeting. J Nucl Med 1999;40(6):1061-1071
31. Provost C, Rozenblum-Beddok L, Nataf V, Merabtene F, Prignon A, Talbot JN. [^{68}Ga]RGD Versus [^{18}F]FDG PET Imaging in Monitoring Treatment Response of a Mouse Model of Human Glioblastoma Tumor with Bevacizumab and/or Temozolomide. Mol Imaging Biol. 2019;21(2):297-305.
32. Rasmussen T, Follin B, Kastrup J, et al. Angiogenesis PET Tracer Uptake (^{68}Ga-NODAGA-E[(cRGDyK)]) in Induced Myocardial Infarction and Stromal Cell Treatment in Minipigs. Diagnostics (Basel). 2018;8(2):33.
33. Yan B, Fu T, Liu Y, et al. ^{99m}Tc-3PRGD2 single-photon emission computed tomography/computed tomography for the diagnosis of choroidal melanoma: A preliminary STROBE-compliant observational study. Medicine (Baltimore). 2018;97(40):e12441.
34. Zhu Z, Miao W, Li Q, Dai H, Ma Q, Wang F, et al. 99mTc-3PRGD2 for integrin receptor imaging of lung can- cer: a multicenter study. J Nucl Med 2012; 53(5):716–722.
35. Jin X, Liang N, Wang M, Meng Y, Jia B, Shi X, et al. Integrin Imaging with ^{99m}Tc-3PRGD2 SPECT/CT Shows High Specificity in the Diagnosis of Lymph Node Metastasis from Non-Small Cell Lung Cancer. Radiology. 2016;281(3):958-966.
36. Jin X, Zheng K, Shi X,Jia B,Dong C, Zheng L, et al. ^{99}Tc^{m}-3PRGD$_2$for Integrin Receptor Imaging of Pancreatic Cancer: Experimental Study on Tumor Bearing Nude Mice and Clinical Transformation Research. JOURNAL OF NUCLEAR AND RADIOCHEMISTRY, 2020, 42(3): 161-166.
37. Siegel RL, Miller KD, Jemal A. Cancer statistics, 2020. CA Cancer J Clin 2020; **70:** 7–30.
38. American Cancer Society. Cancer Facts & Figures 2020. Atlanta, GA: American Cancer Society, 2020.
39. Mizrahi JD, Surana R, Valle JW, Shroff RT. Pancreatic cancer.Lancet. 2020;395(10242):2008-2020.
40. Xiong HQ, Rosenberg A, LoBuglio A, Schmidt W, Wolff RA, Deutsch J, et al. Cetuximab, a monoclonal antibody targeting the epidermal growth factor receptor, in combination with gemcitabine for advanced pancreatic cancer: a multicenter phase II Trial. J Clin Oncol. 2004;22(13):2610–6.
41. Kindler HL, Friberg G, Singh DA, Locker G, Nattam S, Kozloff M, et al. Phase II trial of bevacizumab plus gemcitabine in patients with advanced pancreatic cancer. J Clin Oncol. 2005;23(31):8033–40.
42. Tian W, Ding W, Kim S, Xu X, Pan M, Chen S. Efficacy and safety profile of combining agents against epidermal growth factor receptor or vascular endothelium growth factor receptor with gemcitabine-based chemotherapy in patients with advanced pancreatic cancer: a meta-analysis. Pancreatology. 2013;13(4): 415–22.
43. Yang Z, Kang M, Zhu S, Huang J, Li X, Wang R. Clinical evaluation of vascular normalization induced by recombinant human endostatin in nasopharyngeal carcinoma via dynamic contrast-enhanced ultrasonography. Onco Targets Ther. 2018;11:7909-7917.

44. Inai T, Mancuso M, Hashizume H, Baffert F, Haskell A, Baluk P, et al. Inhibition of vascular endothelial growth factor (VEGF signaling in cancer causes loss of endothelial fenestrations, regression of tumor vessels, and appearance of basement membrane ghosts. Am J Pathol 2004;165(1):35-52.
45. Rofstad EK, Gaustad JV, Egeland TA, Mathiesen B, Galappathi K .Tumors exposed to acute cyclic hypoxic stress show enhanced angiogenesis, perfusion and metastatic dissemination. Int J Cancer .2010;127(7):1535–1546.
46. Wang WQ, Liu L, Sun HC, Fu YL, Xu HX, Chai ZT, et al. Tanshinone IIA inhibits metastasis after palliative resection of hepatocellular carcinoma and prolongs survival in part via vascular normalization. J Hematol Oncol. 2012;5:69.
47. Zhang H, Ren Y, Tang X, Wang K, Liu Y, Zhang L, et al. Vascular normalization induced by sinomenine hydrochloride results in suppressed mammary tumor growth and metastasis. Sci Rep 2012; 5:69.
48. Van den Eynden GG, Bird NC, Majeed AW, Van Laere S, Dirix LY, Vermeulen PB.The histological growth pattern of colorectal cancer liver metastases has prognostic value. Clin Exp Metastasis. 2012;29(6):541–549.
49. Jain RK. Normalizing tumor vasculature with anti-angiogenic therapy: a new paradigm for combination therapy. Nat Med. 2001;7(9): 987–989.
50. Lin MI, Sessa WC. Antiangiogenic therapy: creating a unique “window” of opportunity. Cancer Cell. 2004;6(6):529–531.
51. Xu Q, Gu J, Lv Y, Yuan J, Yang N, Chen J,, et al. Angiogenesis for tumor vascular normalization of Endostar on hepatoma 22 tumor-bearing mice is involved in the immune response. Oncol Lett. 2018;15(3):3437-3446.
52. Yang Z, Kang M, Zhu S, Huang J, Li X, Wang R. Clinical evaluation of vascular normalization induced by recombinant human endostatin in nasopharyngeal carcinoma via dynamic contrast-enhanced ultrasonography. Onco Targets Ther. 2018;11: 7909-7917.

Tables

Table 1 Unpaired t-test(treatment groups vs control group)

Time / Groups	Day 0		Day 7		Day 14		Day 21		Day 28	
	Tumor Volume	T/NT	Tumor Volume	T/NT	Tumor Volume	T/NT	Tumor Volume	T/NT	Tumor Volume	T/NT
Endostar vs Control	P=0.953	P=0.573	P=0.696	P=0.033	P=0.143	P□0.01	P=0.07	P=0.015	P□0.01	P□0.01
Gemcitabine vs Control	P=0.917	P=0.630	P=0.441	P=0.108	P=0.258	P□0.01	P=0.191	P=0.041	P=0.023	P=0.044
Endostar + Gemcitabine vs Control	P=0.959	P=0.769	P=0.136	P□0.01	P□0.01	P□0.01	P□0.01	P□0.01	P□0.001	P□0.01

Table 2 Repeated measurement AVONA				
AVONA	Tumor Volume		T/NT	
Groups	F	P	F	P
Endostar vs Control	5.660	0.035	12.981	0.004
Gemcitabine vs Control	4.899	0.047	6.913	0.022
Endostar + Gemcitabine vs Control	11.873	0.005	16.133	0.002
Gemcitabine vs Endostar + Gemcitabine	7.086	0.021	11.838	0.005
Endostar vs Gemcitabine	0.047	0.832	4.955	0.051
Endostar vs Endostar + Gemcitabine	5.735	0.034	0.302	0.593

Figures

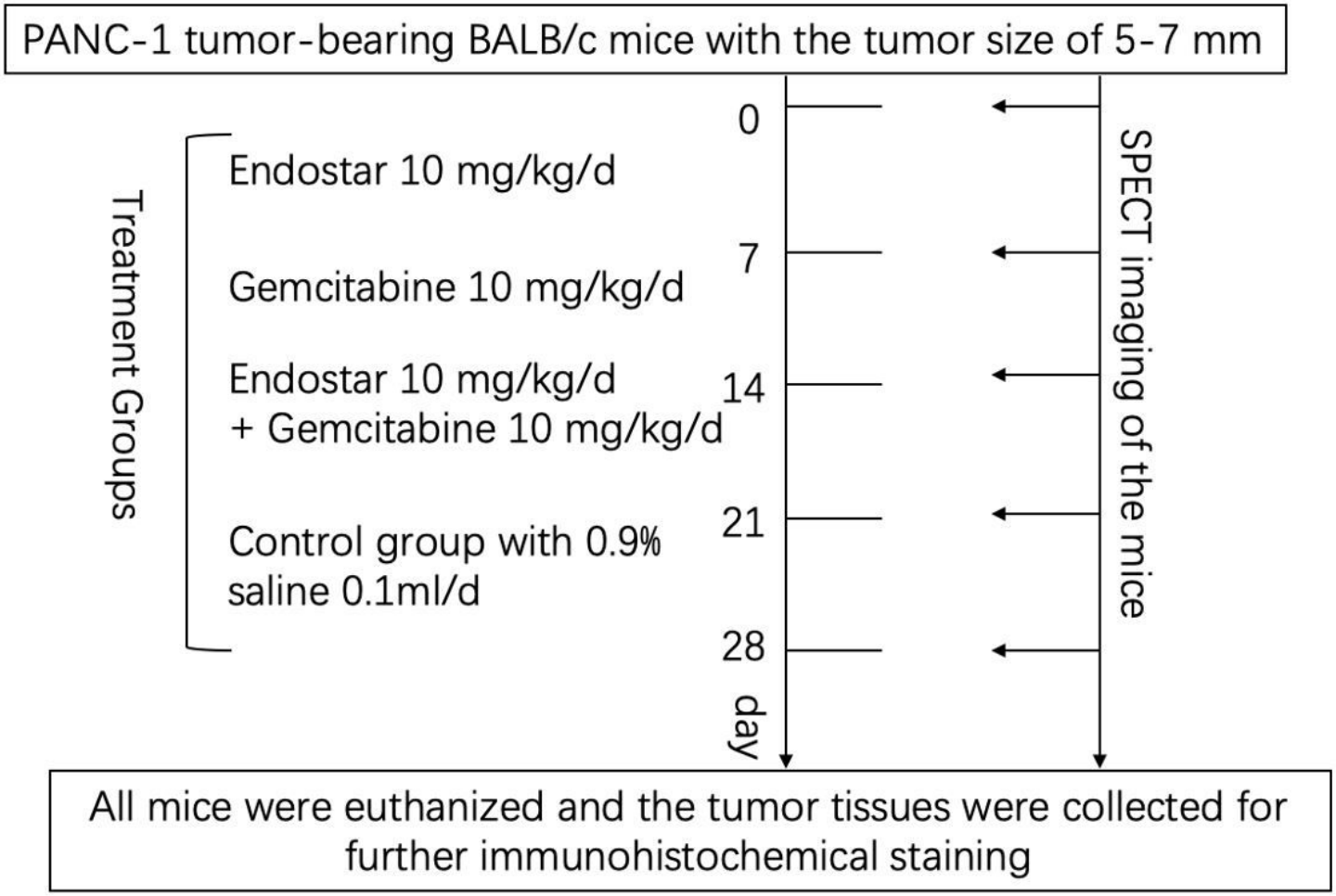

Figure 1

Therapy and imaging protocol

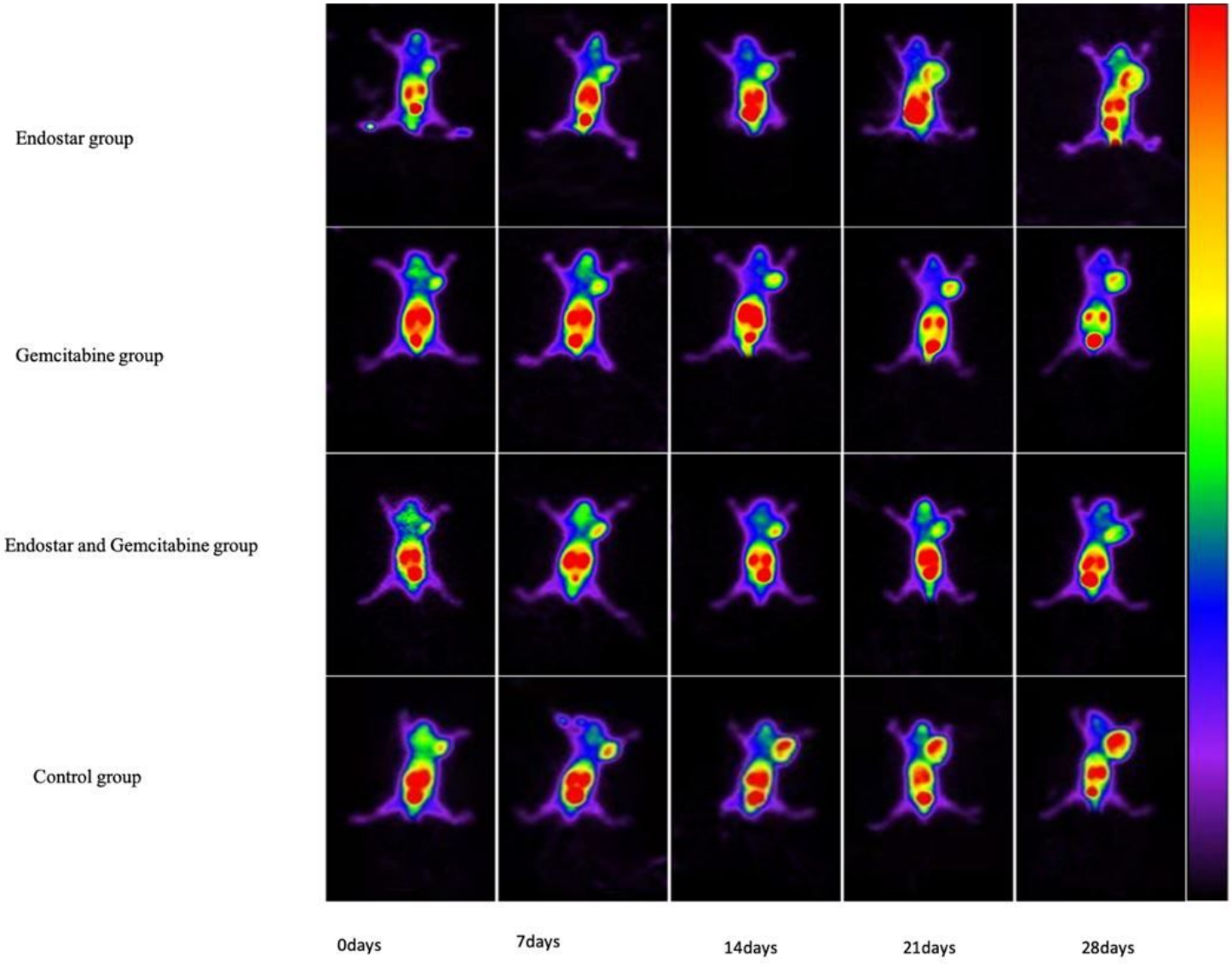

Figure 2

99mTc-3PRGD2 SPECT in Endostar、Gemcitabine、the combination of those two agents and the control group.PANC-1 tumor bearing mice at days 0, 7, 14, 21and28 post-treatment.

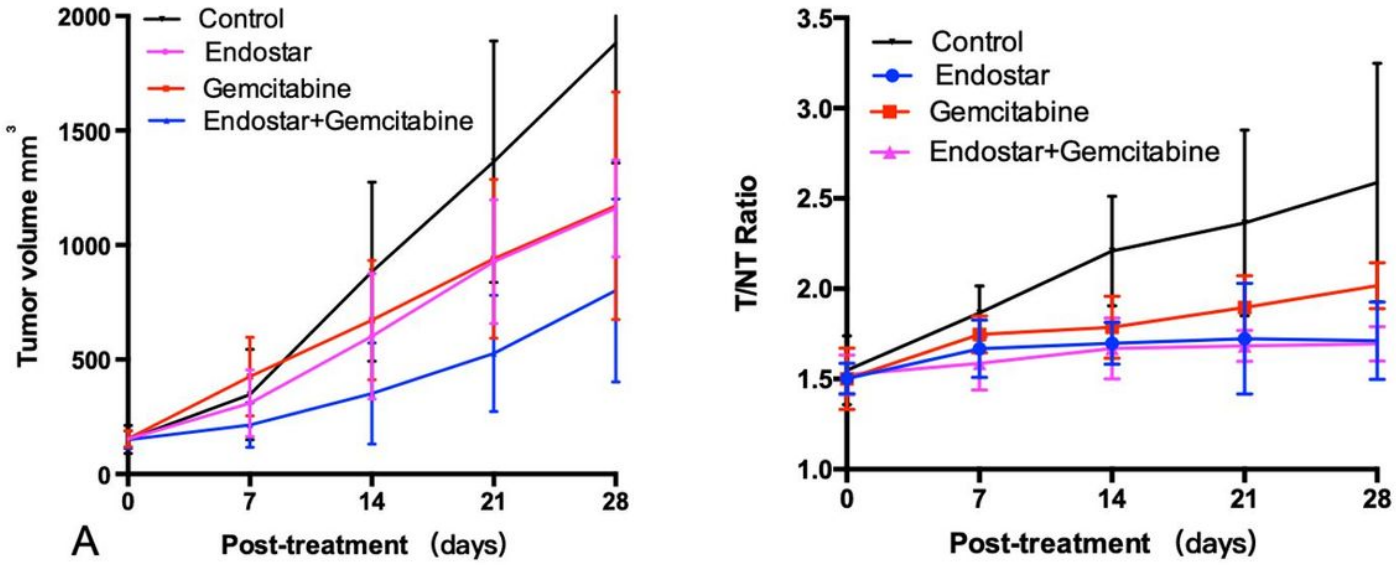

Figure 3

Tumor growth profiles of control group and treatment groups (7 mice per group). PANC-1 tumors bearing mice were treated with via intraperitoneal injection. Saline-treated animals served as controls. B□99mTc-3PRGD2 tumor uptake□T/N□in the groups.

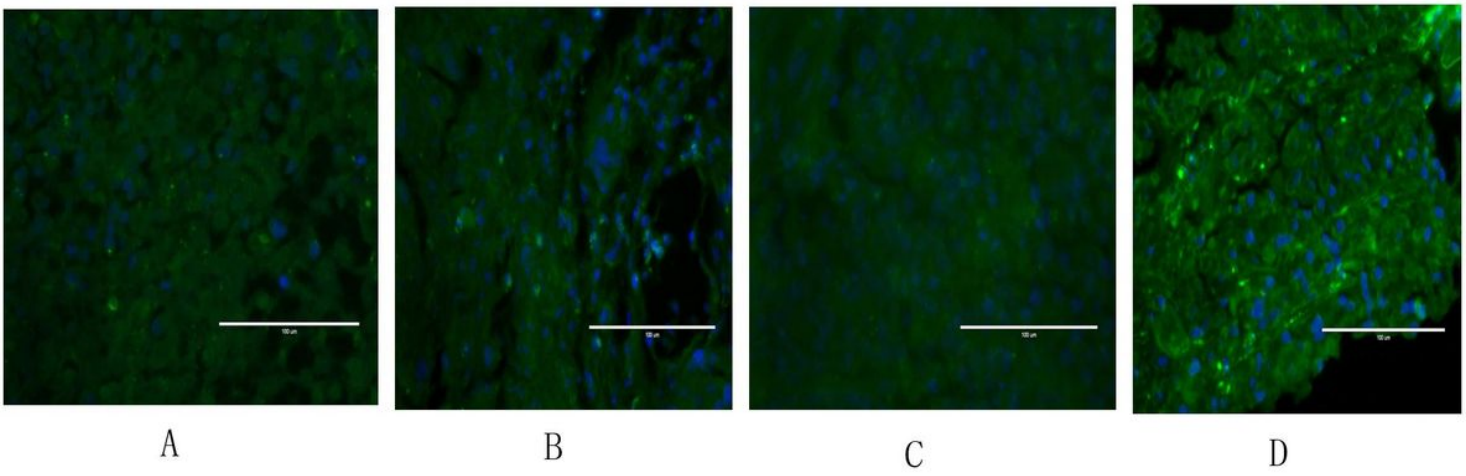

Figure 4

MVD in Endostar(A)□Gemcitabine(B)□the combination of those two agents(C) and the control group(D).